J. Fluid Mech. (1978), *vol.* 88, *part* 1, *pp.* 161–180
Printed in Great Britain

Nonlinear resonant excitation of a long and narrow bay

By STEVEN R. ROGERS
Department of Applied Mathematics, Weizmann Institute of Science, Israel
AND CHIANG C. MEI
Department of Civil Engineering, Massachusetts Institute of Technology, Cambridge

(Received 29 July 1977 and in revised form 19 January 1978)

A nonlinear study of harbour resonance is carried out for a rectangular bay indented from a straight coast. Boussinesq equations with nonlinearity and dispersion are used. Simplifying approximations are made for a narrow bay to decouple the nonlinear problem in the bay from the approximately linear problem in the ocean. Harmonic generation in the bay is studied numerically. Experiments for three different bay lengths and three amplitudes are compared with the numerical theory. The relative importance of entrance loss and boundary-layer dissipation to nonlinearity is estimated.

1. Introduction

Oscillations in a harbour due to an incident wave have been extensively studied in the framework of inviscid linearized long-wave theory (see the review by Miles 1974). Based on the same approximation, effective numerical methods have also been developed for harbours of arbitrary shape but constant depth by using integral equations (Lee 1971; Hwang & Tuck 1970) and for arbitrary shape and depth by using finite elements (Berkhoff 1972; Chen & Mei 1974). For a sufficiently narrow harbour entrance these theories all predict resonant responses within the harbour near the first few natural frequencies of the closed basin. For an incident wave of modest amplitude, the predicted amplification at resonance can often be so high (by a factor of 10, say) as to invalidate the assumption of linearity. For constant depth excellent experiments have been performed by Lee in very deep water; the results have been used to confirm the linearized shallow-water theory by invoking its mathematical analogy with the deep-water theory. However, nonlinear effects are demonstrably more important in shallow than in deep water; hence the good agreement between the linearized shallow-water theory and a deep-water experiment is not necessarily a decisive confirmation of the former. Although real-fluid effects (which are difficult to estimate precisely) can be called upon to reduce the large amplification predicted by a linear theory, it is still useful to know when and whether nonlinearity may play a more important role.

A study of certain nonlinear effects in a narrow rectangular bay connected to a wider channel has recently been made by Bowers (1977). The purpose there was to show that the second-order set-down of incident groups of short swells can resonate the bay near the long period of the groups. While the study demonstrated decisively

the resonance mechanism, the width of the channel was so much less than the incident wavelength as to render the problem essentially one-dimensional. Further modification to account for two-dimensional radiation is needed to make Bowers' results directly applicable to harbour resonance.

Nonlinear waves in shallow water have been studied extensively with reference to pure progressive waves and standing waves in a closed basin. A common theoretical basis for all this work has been the Boussinesq equations, which account for both nonlinearity and dispersion to the leading order. For unidirectional propagation, the general theory of an initial-value problem in an infinite space based on the Korteweg–de Vries equation is now well known. These investigations are largely one-dimensional in space.

In this paper a nonlinear theory and corresponding experiments for shallow-water waves will be presented for the two-dimensional problem of a long rectangular bay of small width opened to an infinite ocean. The Boussinesq equations are used as the basis. As an important simplification it will first be argued that the wave radiated away from the narrow opening is small enough to justify a linear approximation in the ocean; thus nonlinearity, which is enhanced by resonance in the bay, is also limited to the bay. The matching of the bay and ocean will be effected approximately in terms of radiation impedances. By comparing the experiments for fixed frequencies and three different bay lengths we shall show that intrinsic nonlinear effects can be secondary to entrance loss only for very short bays, but become dominant for sufficiently long bays.

2. Formulation

2.1. *The Boussinesq equations*

We start from the assumptions of inviscid fluid and irrotational flow. It is well known in the theory of long water waves that the Boussinesq approximation which includes nonlinearity and dispersion to the leading order enjoys a wide range of validity, and therefore it will be used as the basis of our study. The following dimensionless variables will be used:

$$t' = \omega t, \quad (x', y') = (x, y)\,\omega/(gh)^{\frac{1}{2}}, \quad z' = z/h, \quad \zeta' = \zeta/h, \quad \mathbf{u}' = \mathbf{u}/(gh)^{\frac{1}{2}}, \qquad (2.1a\text{–}e)$$

where ω is the characteristic frequency, ζ is the free-surface displacement and $\mathbf{u}(x, y, t)$ is the depth-averaged horizontal velocity. Assuming that the depth h is everywhere constant, the Boussinesq equations take the following form:

$$\left.\begin{aligned} \zeta_t + \nabla.\mathbf{u} + \nabla.(\zeta\mathbf{u}) &= 0, \\ \mathbf{u}_t + \nabla\zeta + \tfrac{1}{2}\nabla\mathbf{u}^2 + \tfrac{1}{3}\mu^2\nabla\zeta_{tt} &= 0, \end{aligned}\right\} \qquad (2.2)$$

where primes have been omitted for brevity. The small parameter, $\mu^2 = \omega^2 h/g \ll 1$, is a measure of frequency dispersion. It is assumed that the dimensionless amplitude of the wave is also small and measured by the small parameter $\epsilon = O(\zeta')$. The error terms in (2.2) are $O(\epsilon^2, \epsilon\mu^2, \mu^4)\,\epsilon$.

The coastline is designated by $x = 0$. The bay is rectangular with physical length

L, width $2a$, and $y = 0$ as its longitudinal axis. In dimensionless variables, the boundary conditions on the solid walls are

$$\mathbf{u}.\mathbf{n} = 0 \begin{cases} \begin{cases} -l < x < 0 & y = \pm\delta \\ x = -l & |y| < \delta \end{cases} & \text{(bay boundaries)}, \\ x = 0 \quad |y| > \delta & \text{(coast line)}, \end{cases} \tag{2.3}$$

where $(l, \delta) = (L, a)\,\omega/(gh)^{\frac{1}{2}}$.

At infinity there are incident waves ζ^i, reflected waves from the coast ζ^r, and radiated waves from the bay opening ζ^R. The precise statement of the radiation condition will be postponed until later.

We recall that the linearized long-wave theory incorporates only the first two terms of each equation in (2.2) and is a valid first approximation for a large spatial region only if $\epsilon/\mu^2 \ll 1$. This condition is frequently violated in natural settings as well as in the laboratory, where a certain minimum amplitude is required for accurate measurement. It should be noted that, if the normalized range of the spatial region is not greater than $O(1)$, then the usual linearized theory is still a good first approximation even for $\epsilon/\mu^2 = O(1)$.

We shall study only incident waves and responses which are periodic in time, with the fundamental circular frequency ω. Let us represent the solutions as Fourier series

$$\begin{matrix} \zeta(x,y,t) \\ \mathbf{u}(x,y,t) \end{matrix} = \tfrac{1}{2}\sum_n \begin{bmatrix} \zeta_n(x,y) \\ \mathbf{u}_n(x,y) \end{bmatrix} \exp(-int), \quad n = 0, \pm 1, \pm 2, \ldots, \tag{2.4}$$

where $(\zeta_{-n}, \mathbf{u}_{-n})$ are equal to the complex conjugates of $(\zeta_n, \mathbf{u}_n)$. It follows from (2.2) that

$$-in\zeta_n + \nabla.\mathbf{u}_n + \tfrac{1}{2}\sum_s \nabla.(\zeta_s \mathbf{u}_{n-s}) = 0, \tag{2.5a}$$

$$-in\mathbf{u}_n + (1 - \tfrac{1}{3}\mu^2 n^2)\nabla\zeta_n + \tfrac{1}{4}\sum_s \nabla(\mathbf{u}_s.\mathbf{u}_{n-s}) = 0, \tag{2.5b}$$

which may be combined to give

$$(\nabla^2 + k_n^2)\zeta_n = \sum_n \left[\frac{-in}{2}\nabla.(\zeta_s \mathbf{u}_{n-s}) - \tfrac{1}{4}\nabla^2(\mathbf{u}_s.\mathbf{u}_{n-s})\right][1 + O(\epsilon^2, \epsilon\mu^2, \mu^4)], \tag{2.6}$$

where

$$k_n^2 = n^2/(1 - \tfrac{1}{3}\mu^2 n^2) = n^2(1 + \tfrac{1}{3}\mu^2 n^2) \tag{2.7}$$

is the approximate dispersion relation.

Although the Fourier series is formally infinite, we anticipate that, in cases where $\epsilon/\mu^2 \leqslant O(1)$, the bay length l is not too great, and the incident waves contain only a few harmonics, only the first few (three or four) harmonics are appreciable in the response. This anticipation underlies most of our subsequent approximations and is confirmed in the numerical results.

2.2. *The linearized result*

To facilitate later discussion we recall the linearized result which is analogous to the organ pipe problem in acoustics. Assuming that the *normally* incident wave consists of only the first harmonic $n = 1$, then for a narrow bay $\delta \ll 1$, the harbour response is one-dimensional except within a distance $O(\delta)$ from the entrance,

$$\left.\begin{aligned} \zeta(x,t) &= \mathrm{Re}\{T_1 \cos k_1(x+l)\exp(-it)\}, \\ u(x,t) &= \mathrm{Re}\{(iT_1/k_1)\sin k_1(x+l)\exp(-it)\}, \end{aligned}\right\} \quad x < 0, \tag{2.8}$$

where

$$\left.\begin{aligned} \tfrac{1}{2}A_1 &= \text{dimensionless amplitude of incident wave},\\ T_1 &= A_1[\cos k_1 l - (iZ_1/k_1)\sin k_1 l]^{-1},\\ Z_1 &= k_1^2\delta[1+(2i/\pi)\ln(k_1\delta\{2\gamma/\pi e\})] = \text{entrance impedance},\\ \ln\gamma &= 0{\cdot}577216\ldots = \text{Euler's constant}. \end{aligned}\right\} \tag{2.9}$$

This result, which differs only slightly from that of Miles & Munk (1961) owing to their approximation at the bay entrance, is deducible by matched asymptotics for small $k_1\delta$ (Ünlüata & Mei 1973). Since $\operatorname{Im}\{Z_1\} = O(\delta\ln\delta)$, the resonant frequencies or bay length are approximately at the zeros of

$$\cos k_1 l + \frac{1}{k_1}(\sin k_1 l)\operatorname{Im} Z_1 = 0, \tag{2.10}$$

or

$$(k_1 l) \cong (m+\tfrac{1}{2})\pi + [(1/k_1)\operatorname{Im} Z_1]_{k_1 l=(m+\frac{1}{2})\pi}. \tag{2.11}$$

At the mth resonant peak the maximum bay response is

$$\max_{(x,\,t)}\zeta = k_1|A_1|\,[(\operatorname{Re} Z_1)\sin k_1 l]^{-1} \sim O(A_1/\delta), \tag{2.12}$$

with k_1 given by (2.7). Since the maximum displacement is defined to be $O(\epsilon)$ we must have $A_1 \sim O(\epsilon\delta)$.

Far from the bay entrance, the total solution in the ocean is given by

$$\zeta(x,y,t) = \tfrac{1}{2}A_1(\exp(ik_1x) + \exp(-ik_1x)) + iT_1k_1\delta\sin k_1 l H_0^{(1)}(k_1 r), \tag{2.13}$$

with

$$r^2 = (x^2+y^2)^{\frac{1}{2}} \gg \delta, \quad x > 0.$$

The maximum amplitude of the radiated wave occurs at resonance and in the near field $r \sim O(\delta)$ of the bay entrance and, except for the immediate neighbourhood of sharp corners, is roughly $\sim \epsilon\delta\ln\delta \ll 1$ upon expanding the Hankel function and using (2.12).

These order estimates based on the first harmonic suggest an important simplification: if nonlinear terms up to $O(\epsilon^2)$ are kept in the bay, nonlinearity in the ocean is at best $O(\epsilon\delta\ln\delta)^2$ and can be ignored. Furthermore, as a practical measure, the same simplification can be extended to the higher harmonics if only the first few harmonics are numerically important. This measure is related to truncation of Fourier series.

2.3. *Governing equations for the ocean and the impedance condition*

In view of the preceding comments we shall drop the nonlinear terms for all harmonics in the ocean $x > 0$; from (2.5) we have

$$-in\zeta_n + \nabla.\mathbf{u}_n = 0, \tag{2.14a}$$

$$-in\mathbf{u}_n + \frac{n^2}{k_n^2}\nabla\zeta_n = 0, \tag{2.14b}$$

which can be combined to give

$$(\nabla^2 + k_n^2)\,\zeta_n = 0, \quad x > 0, \tag{2.15}$$

with k_n given by (2.7). Note from (2.5) that the zeroth harmonic, i.e. the time averages, are: ζ_0 = constant and $\nabla.\mathbf{u}_0 = 0$; both ζ_0 and $\mathbf{u}_0$ may be taken to be zero by redefining the datum.

To satisfy the no-flux boundary condition on the coast and the radiation condition at infinity (that radiated waves are outgoing), we represent ζ_n by

$$\zeta_n = A_n \cos k_n x + \zeta_n^R, \quad x > 0, \tag{2.16a}$$

with

$$\zeta_n^R = \frac{k_n^2}{2n} \int_{-\delta}^{\delta} dy' U_n(y') H_0^{(1)}(k_n(x^2 + (y-y')^2)^{\frac{1}{2}}. \tag{2.16b}$$

The first term on the right of (2.16*a*) is the sum of the incident and the reflected nth harmonic, while ζ_n^R is the radiated nth harmonic. In the integrand of (2.16*b*), $U_n(y)$ is the nth harmonic amplitude of the normal velocity at the bay entrance, and is related to the surface gradient by

$$\frac{\partial \zeta_n^R}{\partial x}(0, y) = \frac{ik_n^2}{n} U_n(y), \quad |y| < \delta, \quad x = 0^+. \tag{2.17}$$

In the bay not close to the entrance, $k_1 r = O(1)$. Since $k_n \delta$ is small for the first few harmonics we may expand the Hankel function to obtain

$$\zeta_n^R = \frac{k_n}{n} \bar{U}_n k_n \delta H_0^{(1)}(k_n r)[1 + O(n\delta)], \quad k_n r = O(1), \tag{2.18}$$

where $\bar{U}_n$ is the average of U_n across the entrance.

Across the entrance, the approximation for small $k_n \delta$ is

$$\zeta_n^R(0, y) = \frac{k_n^2}{n} \left\{ \delta \bar{U}_n + \frac{i}{\pi} \int_{-\delta}^{\delta} dy' U_n(y') \ln\left(\frac{\gamma k_n}{2} |y - y'|\right) + O[(k_n \delta)^2 \ln k_n \delta] \right\}. \tag{2.19}$$

In particular, the average across the entrance of ζ_n^R may be written as

$$\bar{\zeta}_n^R(x = 0) \cong Z_n \bar{U}_n \equiv \bar{U}_n \left\{ \frac{k_n^2 \delta}{n} \left[1 + \frac{2i}{\pi} (\ln k_n \delta + c_n) \right] \right\}, \tag{2.20a}$$

where

$$c_n = \ln \tfrac{1}{2}\gamma + \tfrac{1}{4} \int\int_{-1}^{1} \ln |\nu - \nu'| \frac{U_n(\nu')}{\bar{U}_n} d\nu \, d\nu', \tag{2.20b}$$

which depends, in principle, on the profile of U_n. Combining with the incident and the reflected waves we have at the harbour entrance

$$\bar{\zeta}_n = A_n - \frac{in}{k_n^2} Z_n \frac{\partial \bar{\zeta}_n}{\partial x}, \quad x = 0^+, \tag{2.21}$$

where use is made of (2.17). Z_n can be called the *impedance* of the nth harmonic.

It may be remarked that $\mathrm{Re}\, Z_n \sim O(k_n \delta)$ corresponds to the radiation damping while $\mathrm{Im}\, Z_n \sim O(k_n \delta \ln k_n \delta)$ corresponds to the mass reactance. Only the latter depends directly on the detailed variations of $U_n(y)$. A quasi-steady approximation which is asymptotically correct for small $k_n \delta$ within the inviscid theory leads to

$$Z_n \cong \frac{k_n}{n} (k_n \delta) \left[1 + \frac{2i}{\pi} \ln \frac{2\gamma k_n \delta}{\pi e} \right], \tag{2.22}$$

within the present accuracy (Ünlüata & Mei 1973).

2.4. *Governing equation for the bay*

We first reaffirm a known result in the linearized theory that the wave field in most of the bay is one-dimensional except in the $O(\delta)$ neighbourhood of the entrance. That this is still true in a nonlinear theory can be shown by rescaling y by δ, i.e. by introducing $\mathcal{y} = y/\delta$. It then follows from the governing equations straightforwardly that $\partial\zeta/\partial\mathcal{y}, \partial u/\partial\mathcal{y}, v = O(\delta^2)$. Thus in the far field of the bay (2.4*a*, *b*) become

$$-in\zeta_n + u_n' + \tfrac{1}{2}\sum_s (\zeta_s u_{n-s})' = 0, \tag{2.23a}$$

$$-inu_n + \frac{n^2}{k_n^2}\zeta_n' + \tfrac{1}{2}\sum_s (u_s u_{n-s})' = 0, \tag{2.23b}$$

where primes denote d/dx. After some manipulations, one finds that to the accuracy of the Boussinesq approximation

$$\zeta_n'' + k_n^2\zeta_n = \tfrac{1}{2}\sum_s (n^2 - s^2)\zeta_s\zeta_{n-s} - \tfrac{1}{2}\sum_{s\neq n}\frac{n+s}{n-s}\zeta_s'\zeta_{n-s}', \tag{2.24}$$

which is a set of nonlinear ordinary differential equations.

The boundary conditions are now

$$\zeta_n'(-l) = 0, \quad \text{i.e. } u_n(-l) = 0, \tag{2.25}$$

at the landward end of the bay.

Across the bay entrance, ζ and $\partial\zeta/\partial x$ must be continuous, implying that the condition (2.21) should be satisfied by the bay solution as well. We now take Z_n to be given by (2.22), which corresponds to using the quasi-steady approximation for $U_n(y)$, and impose (2.21) directly on the far-field solution of (2.24) in the bay, i.e.

$$\zeta_n = A_n - \frac{in}{k_n^2} Z_n \frac{\partial\zeta_n}{\partial x}, \quad x = 0^-, \tag{2.26}$$

which will be referred to as the *impedance condition*. Thus continuity across the bay entrance is satisfied in an averaged sense.

In summary, through the impedance condition, the ocean and the bay are decoupled. In the bay one has a two-point boundary-value problem for a set of nonlinearly-coupled second-order ordinary differential equations (2.24) subject to the boundary conditions (2.25) and (2.26). After its solution the approximate ocean response follows from (2.13). It can be shown that in the linearized limit this procedure leads to the same result by a matched asymptotic analysis (Ünlüata & Mei 1973), and to almost the same results if other guesses are made for the profile of $U_1(y)$.

3. The solution

3.1. *Remarks on the mean sea level*

The phenomenon of a spatially varying mean sea level due to nonlinearity is known in simpler wave states (e.g. for pure progressive and standing waves, see Longuet-Higgins & Stewart 1964). In the bay under study it corresponds to the zeroth har-

monic ($n = 0$) and can be found directly by integrating (2.23). Using (2.25) and assuming $A_0 = 0$ it can be easily shown that

$$\zeta_0(x) = \tfrac{1}{4} \sum_s (|u_s(0)|^2 - |u_s(x)|^2), \tag{3.1}$$

which gives the mean sea level inside the bay. In particular, at the entrance $\zeta_0(0) = 0$; while at the end of the bay, $u_s(x) = 0$, so that $\zeta_0(-l)$ is a maximum *set-up*

$$\zeta_0(-l) = \tfrac{1}{4} \sum_s |u_s(0)|^2 > 0. \tag{3.2}$$

On a frequency response plot the peaks of this mean set-up are expected to coincide with the resonant peaks of the first few harmonics.

As a matter of computation we note that $\zeta_0 = O(\epsilon^2)$, so that the zeroth harmonic can be omitted in calculating all other harmonics, and can be obtained after the latter are known.

We also observe from (2.23a) that u_0 is at best $O(\epsilon^2)$. In fact, the following argument restricts u_0 still further. Multiplying (2.23a) by ζ_{-n} and (2.23b) by $u_{-n} k_n^2/n^2$, summing over n and adding the two resulting equations, we have

$$\sum_s -in \left(|\zeta_n|^2 + \frac{k_n^2}{n^2} |u_n|^2 \right) + \sum (\zeta_n u_n)' = O(\epsilon^3).$$

Replacing the index n by $-p$, it is easily seen that the first series equals its own negative, hence is zero. It follows that

$$\sum_s (\zeta_n u_{-n})' = O(\epsilon^3),$$

which upon integrating (2.23a) implies that $u_0 = O(\epsilon^3)$ and is therefore negligible in (3.1).

3.2. *A second-order approximation*

In order to provide checks for later numerical work and to assist in physical understanding we have worked out a second-order theory by regular perturbations. The starting assumptions are that $\epsilon/\mu^2 < O(1)$ and arbitrary l, but the results are also valid for $\epsilon/\mu^2 = O(1)$ if $l \leqq O(1)$, which applies to the practically important case of the quarter-wavelength mode. The incident wave consists of the first harmonic only. The analysis is straightforward and is omitted here. While the first harmonic is still given by § 2.2, the mean sea level is

$$\zeta_0(x) = \frac{1}{4k_1^2} |T_1|^2 [\cos 2k_1(x+l) - \cos 2k_1 l]. \tag{3.3}$$

The second harmonic is

$$\zeta_2 = \tfrac{3}{2} T_1^2 \left\{ g(x) - \frac{g(0) + \dfrac{2i}{k_2^2} Z_2 g'(0)}{\cos k_2 l - \dfrac{2i}{k_2} Z_2 \sin k_2 l} \cos k_2(x+l) + O(\mu^2) \right\}, \tag{3.4a}$$

with

$$g(x) = \tfrac{1}{4}(x+l) \sin k_2(x+l). \tag{3.4b}$$

The behaviour of ζ_1 is well known, while ζ_0 has resonant peaks at the same values of l as the peaks of ζ_1 through T_1. We only present in figure 1 the behaviour of $\zeta_2(-l)$ at

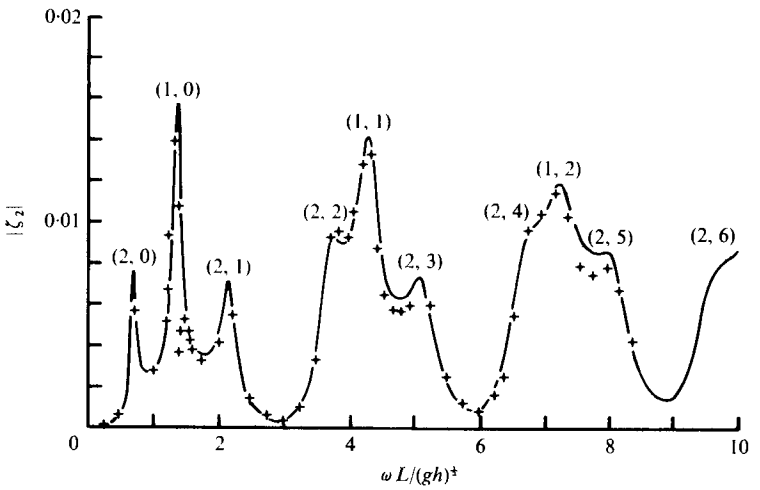

FIGURE 1. Second harmonic amplitude at the back wall. Input data are: $h = 20\,\text{m}$, $2a = 100\,\text{m}$, $L = 1000\,\text{m}$, $A_1 = 0{\cdot}03$. ——, by equation (2.4); +, by numerical theory of §4. Differences are appreciable only near high peaks.

the end of the bay which has the dimensions $a = 50\,\text{m}$, $h = 20\,\text{m}$, and $L = 1000\,\text{m}$. The incident first harmonic is chosen to be $A_1 = 0{\cdot}03$. The peaks can be identified with the help of (3.4a). There are two sets of resonant peaks. One set corresponds to the maxima of T_1, i.e. the resonant peaks of the first harmonic which are near $(m+\frac{1}{2})\pi$, $m = 0, 1, 2, \ldots$; these peaks are labelled by (1, 0), (1, 1), (1, 2), etc. The second set corresponds to the maxima of the second term in (3.4a), i.e. the resonant peaks of the second harmonic which are near $(m+\frac{1}{2})\frac{1}{2}\pi$; these peaks are labelled by (2, 0), (2, 1), (2, 3) ..., etc. A better approximation for the position of the peaks is given by a formula similar to (2.11):

$$l_{nm} = \frac{(m+\frac{1}{2})\pi}{n(1+\frac{1}{8}\mu^2 n^2)}\left[1 - \frac{2}{\pi}\frac{\delta}{l}\ln\frac{el}{2\gamma(m+\frac{1}{2})\delta}\right], \tag{3.5}$$

which shows that the peaks are shifted to the left of their crude estimates. The shift increases with m, n and dispersion μ^2. Since some neighbouring peaks can be very close, the amplification of ζ_2 can be compounded.

3.3. *Numerical method*

We shall apply a numerical method to solve for ζ_n directly from (2.24), (2.25) and (2.26). This method is straightforward and is workable as long as the number of higher harmonics is not large. In computations the second form of (2.7) is used which is closer to the exact linear dispersion relation. The infinite set of two-point boundary-value problems can be truncated after $n = N$ and solved by iteration. The truncated set is quasi-linearized so that at the $(p+1)$th iteration the right-hand side of (2.24) is replaced by

$$\sum_s \left[R_{ns}\zeta_s^{(p)}\zeta_{n-s}^{(p+1)} + S_{ns}\zeta_n^{(p)\prime}\zeta_{n-s}^{(p+1)\prime}\right],$$

with

$$R_{ns} = \tfrac{1}{2}(n^2 - s^2), \quad S_{ns} = -\frac{1}{2}\frac{n+s}{n-s}. \tag{3.6}$$

The resulting linear two-point problems for $\zeta_n^{(p+1}$ are then solved by the method of complementary functions (see Young & Gregory 1973, vol. 2, p. 579 ff.; or Roberts & Shipman 1972, pp. 50 ff. for more extensive discussions). Thus we introduce the complementary functions $e_n(x, q)$ which are defined by the initial-value problems:

$$e_n'' + k_n^2 e_n = \sum_s R_{ns} \zeta_s^{(p)} e_{n-s} + \sum S_{ns} \zeta_s^{(p)'} e_{n-s}', \quad -l < x < 0,$$

$$e_n'(-l, q) = 0,$$

$$e_n(-l, q) = \begin{cases} 1 & \text{if} \quad n = q, \\ 0 & \text{if} \quad n \neq q, \end{cases} \tag{3.7}$$

which can be solved by stepwise integration. Afterwards we represent the solution for $\zeta_n^{(p+1)}$ by superposition,

$$\zeta_n^{(p+1)} = \sum_{p=1}^{N} \alpha_q e_n(x, q), \tag{3.8}$$

which clearly satisfies the boundary condition (2.25). Now the coefficients α_q must be chosen to satisfy the impedance conditions (2.26); thus we get

$$\sum_{q=1}^{N} \left[e_n(0, q) + \frac{in}{k_n^2} Z_n e_n'(0, q) \right] \alpha_q = A_n, \quad n = 1, 2, 3, \ldots, N, \tag{3.9}$$

which may be solved for α_q. In executing the stepwise integration, we use backward differences for the first derivatives on the right-hand side of (3.7*a*) and central differences for the second derivative on the left. The use of backward differences on the right-hand side increases the truncation error from $O(\Delta x)^2$ to $O(\Delta x)$, but has the advantage of increasing the efficiency of the computational algorithm by uncoupling the N equations for $e_n(x_j)$, $n = 1, 2, \ldots, N$, at each mesh point x_j. Besides, the term $e_n(x_j)$ on the left is replaced by $\frac{1}{2}[e_n(x_{j-1}) + e_n(x_{j+1})]$ to improve stability. Uniform intervals along $-l < x < 0$ are taken such that the step size satisfies $k_N \Delta x = 2\pi/10$, i.e. x is one-tenth of the wavelength of the highest harmonic.

The above procedure is repeated for further iterations until

$$\max_x |\zeta_n^{(p+1)} - \zeta_n^{(p)}| < 0{\cdot}001$$

for all $n = 1, 2, 3, \ldots, N$. The rate of convergence of successive iterates is found to improve significantly by introducing a relaxation parameter λ, i.e. by taking the solution after the $(p+1)$th iteration to be

$$\lambda \zeta_n^{(p+1)} + (1 - \lambda) \zeta_n^{(p)} \quad (\lambda > 0),$$

instead of simply $\zeta_n^{(p+1)}$. Usually the most rapid convergence is achieved with $\lambda \simeq 0{\cdot}5$. After the last iteration, we check whether $\max_x (\zeta_N(x)) < 0{\cdot}001$, otherwise a larger N is taken and iteration repeated.

For all the results to be reported, the fourth harmonic is generally negligible, but N is taken to be 5 in the computations as a precautionary measure. Results will be discussed later. To check the computer program we have made a comparison with the second-order theory for $A_1 = 0{\cdot}03$ and excellent agreement is obtained for the first three harmonics $n = 0, 1, 2$, except near the resonant peaks, see figure 1.

4. Experiments

4.1. *General description*

Experiments have been performed in a wave tank which is 25 ft wide, 45 ft long and 1·5 ft deep. The basin is lined with a smooth plastic sheet on the bottom. The coastline spans the full width of the tank while the bay opens along the longitudinal axis of the tank. The width of the bay is 4 in. while the length is adjustable by a movable end wall. All walls of the bay and of the coast are vertical sheets of marine plywood which are sealed at the construction joints and at the tank bottom. The two sides of the tank are inclined at a slope of 1 : 5 and covered with a 4 in. layer of rubberized horse hair. The wave maker is an aluminium flap of length 25 ft parallel to, and at a distance of 31 ft from, the coast. A water depth of 6 in. was maintained throughout. Wave gauges are of parallel-wire resistance type. Signals were displayed on a Sanborn recorder and at the same time Fourier analysed by a Hewlett–Packard computer with a sampling rate of 14 counts/s. Measurements were taken at 2 in. intervals along the centre-line of the bay, and at 3 in. intervals along the longitudinal axis of the ocean.

The experiments were conducted for a fixed wave period of 1·545 s, but for three different incident wave amplitudes and three different bay lengths which correspond to the first three resonant peaks of the fundamental harmonic. Only one measurement is taken for a given set of parameters, so that no information is available regarding experimental scatter.

Before presenting the experiment results in the harbour, we first examine below two modelling effects not accounted for thus far.

4.2. *Effective size of the ocean*

An important concern in all harbour experiments is the size of the ocean, which must be effectively infinite to avoid spurious resonances. The tank sides perpendicular to the coast are capable of absorbing nearly 80% of incident plane waves of 1·545 s period and therefore cause little reflexion. To evaluate the effect of the highly reflective wave maker we consider the linearized problem of a radiating source of strength Q at $x = 0$, $y = 0$ on one side of an infinite channel of physical width L_m equal to the model ocean length. By the method of images one gets the total *correction* due to the presence of the stationary wall at $x = l_m$,

$$\zeta_c(x, y) = Q \sum_{n=1}^{\infty} [H_0^{(1)}(|\mathbf{r} - 2nl_m\,\mathbf{e}_x|) + H_0^{(1)}(|\mathbf{r} + 2nl_m\,\mathbf{e}_x|)], \tag{4.1}$$

where $l_m = \omega L_m/(gh)^{\frac{1}{2}}$. The primary source $QH_0^{(1)}(r)$ in an infinite ocean and the standing wave must be added to give the total wave field in the model ocean. In particular, along the axis $y = 0$, which is the longitudinal axis of the model ocean,

$$\zeta_c(x, 0) = E(-x) + E(x), \tag{4.2a}$$

where

$$E(x) \equiv Q \sum_{n=1}^{\infty} H_0^{(1)}(2nl_m + x) \quad (0 < x < l_m). \tag{4.2b}$$

For $l_m \gg 1$, we follow Morse & Feshbach (1953, pp. 815 ff.) by keeping the leading asymptotic term of each Hankel function and further approximating the series by

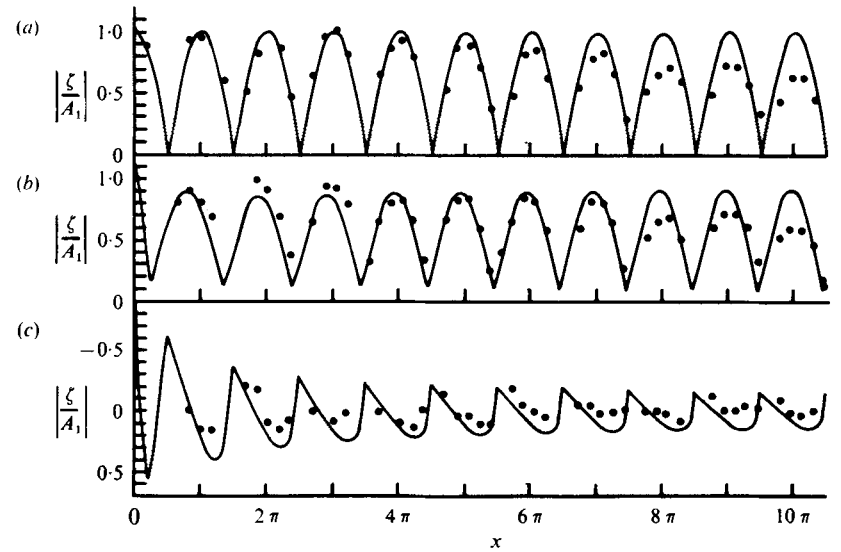

FIGURE 2. Experiment (●) *vs.* theory (——) for the wave amplitude in the ocean ($h = 0{\cdot}5$ ft, $2a = 0{\cdot}33$ ft, $L = 1{\cdot}211$ ft, $\omega = 4{\cdot}067\,\mathrm{s}^{-1}$, $L_m = 31{\cdot}17$ ft, $A_1 = 0{\cdot}040$). (*a*) Harbour closed. (*b*) Harbour open. (*c*) The radiated wave.

an integral (provided $l_m/\pi \neq$ integer, so that the series converges)

$$E(x) \simeq \frac{(2i)^{\frac{1}{2}}}{\pi^{\frac{1}{2}}} Q \exp(ix) \sum_{n=1}^{\infty} \frac{\exp(2inl_m)}{(2nl_m + x)^{\frac{1}{2}}} \simeq \frac{(2i)^{\frac{1}{2}}}{\pi^{\frac{1}{2}}} Q \exp(ix) \int_1^{\infty} d\nu \frac{\exp(i2l_m\nu)}{(2l_m\nu + x)^{\frac{1}{2}}},$$

which can be estimated by partial integration to be

$$E(x) \simeq \frac{(2i)^{\frac{1}{2}}}{\pi^{\frac{1}{2}}} Q \exp(ix) \left\{ \frac{i \exp(2il_m)}{2l_m(2l_m + x)^{\frac{1}{2}}} \right\} + O(l_m^{-\frac{3}{2}}). \tag{4.3}$$

Thus the correction due to the finite model length gives rise to a wave which attenuates at a fast rate of $O(l_m)^{-\frac{3}{2}}$ for any x within $(0, l_m)$ owing to destructive interference among the image sources.

In our experiments, $l_m = 10{\cdot}49\pi$, so that the correction term should be quite negligible. A typical comparison between the measured free-surface amplitude along $y = 0$ and the linearized theory for an infinite ocean is shown in figure 2. A_1 is the measured standing wave amplitude at the point ($x = 0$, $y = 0$) when the bay entrance is closed and is equal to 0·040. In particular, figure 2 (*b*) shows the results when the bay is at the first mode of resonance. The agreement between the linearized theory for an infinite ocean appears good, especially within a wavelength of the bay entrance. Similar comparisons for two smaller amplitudes $A_1 = 0{\cdot}015$ and 0·027 show the same sort of agreement which therefore lends support to the theoretical simplifications for the ocean and the approximate infinity of the laboratory ocean.

4.3. *Real-fluid effects*†

Unlike tests performed in deep water, the bottom of the bay contributes as much viscous damping as the side walls. According to the experiments of Collins (1963) for

† Throughout § 4.3 all variables have physical dimensions.

$\lvert A_1\rvert$	0·015	0·027	0·040
$\lvert A_2\rvert$	0·001	0·003	0·012
$\lvert A_3\rvert$	0·0002	0·001	0·003
$\phi_2 - 2\phi_1$	6·210	5·646	5·506
$\phi_3 - 3\phi_1$	0·671	1·795	5·314

TABLE 1. Measured harmonics at $x = 0$, $y = 0$ when bay is closed.

simple propagating waves, the oscillatory boundary layer remains laminar so long as $u\delta_v/\nu < 160$ where u is the inviscid orbital velocity just outside the boundary layer, ν is the laminar viscosity, and $\delta_v = (2\nu/\omega)^{\frac{1}{2}}$ is the thickness of the boundary layer. For long waves $u = A(gh/h)^{\frac{1}{2}}$. Using the model values $h = 0{\cdot}5\,\text{ft}$, $\omega = 4{\cdot}067\,\text{s}^{-1}$, $\nu = 10^{-5}\,\text{ft}^2/\text{s}$ we find the criterion for laminarity to be $A/h < 0{\cdot}18$, which is satisfied in all but one of our test cases. Therefore, laminar flows prevailed along the walls of the bay.

By estimating the power loss from the boundary layers along the bay walls and the separation loss at the sharp corners of the entrance, the theoretical first harmonic response can be corrected in order to compare with the experimental values. The specifics are rather standard and are described in the appendix for convenience.

5. Results and discussions

We have performed experiments for three bays of lengths $L = 1{\cdot}211$, $4{\cdot}173$ and $7{\cdot}136\,\text{ft}$ which correspond to the first three resonant peaks of the first harmonic with a fixed frequency $\omega = 4{\cdot}067\,\text{s}^{-1}$. These lengths were determined experimentally. For each bay three different amplitudes were tested. The amplitude of the standing waves at $x = 0, y = 0$ when the bay was completely sealed were measured to be $A_1 h = 0{\cdot}0075$, $0{\cdot}0135$ and $0{\cdot}020\,\text{ft}$. Thus the numerical values of the governing dimensionless parameters are

$$l = L\omega/(gh)^{\frac{1}{2}} = 1{\cdot}227,\ 4{\cdot}230 \text{ and } 7{\cdot}233,$$

$$\delta = a\omega/(gh)^{\frac{1}{2}} = 0{\cdot}169,$$

$$\mu^2 = \omega^2 h/g = 0{\cdot}257,$$

$$\lvert A_1\rvert = 0{\cdot}015, 0{\cdot}027 \text{ and } 0{\cdot}040.$$

Physical limitations of the tank made it necessary to use a wavelength of about 6 ft, thus the dispersion parameter μ^2 is probably larger than the Boussinesq approximation tolerates. From measurements, the standing waves at $x = 0$, $y = 0$ also contained some high harmonics whose amplitudes and phase differences with respect to the first harmonic are listed in table 1. These data were used as input for the numerical theory. In all experiments the zeroth harmonics were removed from Fourier analysis since no special care in the experiments was made to ascertain the datum. No visible variation across the bay was noticed.

The first three harmonics from the experiments and the inviscid numerical theory are shown in figure 3 for $l = 1{\cdot}227$, figure 4 for $l = 4{\cdot}230$ and in figure 5 for $l = 7{\cdot}233$. It may be noted that for the smallest $A_1 = 0{\cdot}015$ and the shortest bay, the inviscid linearized theory is quite satisfactory. For a fixed bay, increasing A_1 has the effect

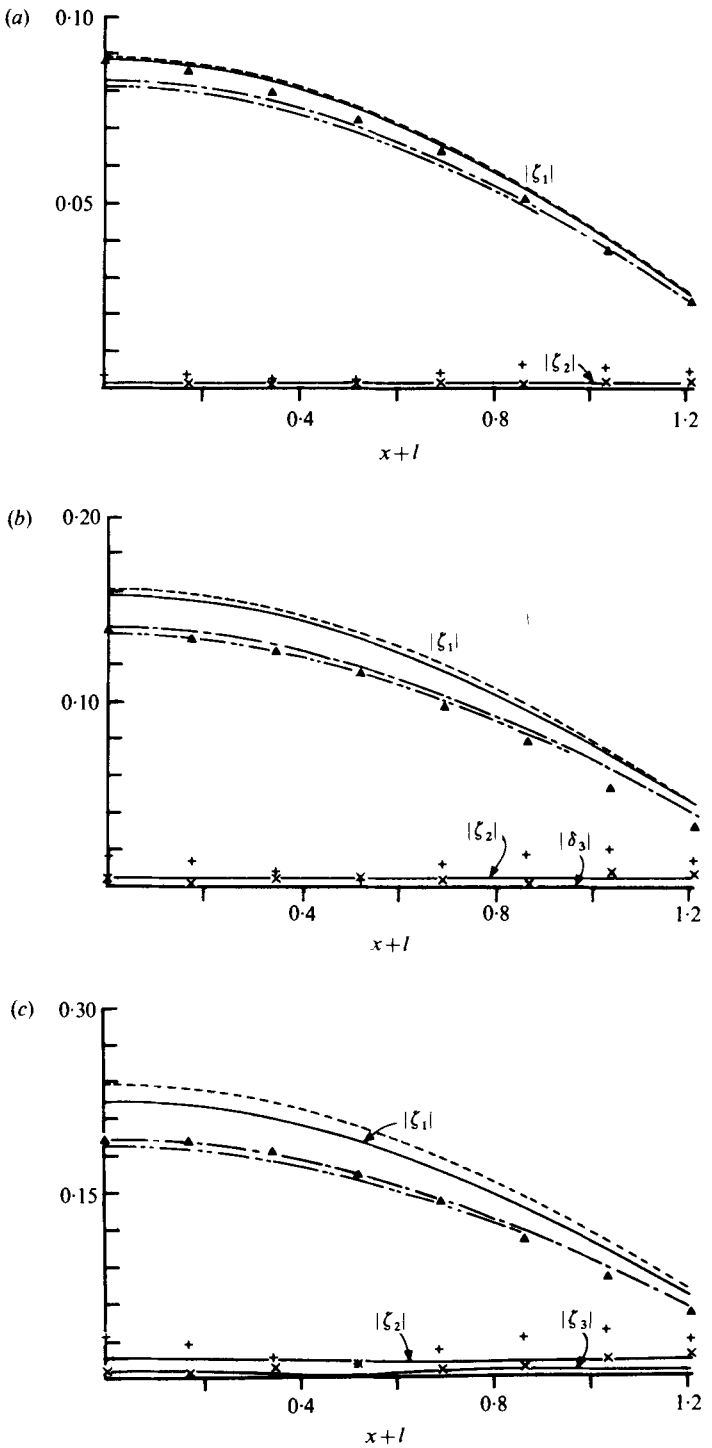

FIGURE 3. (*a*) Experiment *vs.* inviscid nonlinear theory ($f = 0$). ▲, +, ×, measured first, second and third harmonic amplitudes; ——, nonlinear theory; – – – –, linear theory for first harmonic amplitude; — · — · —, first harmonic corrected for entrance loss; — · · — · · —, first harmonic corrected for entrance and boundary layer losses. $L = 1{\cdot}211$ ft, $A_1 = 0{\cdot}015$. (*b*) $L = 1{\cdot}211$ ft, $A_1 = 0{\cdot}027$ (see figure 3*a*). (*c*) $L = 1{\cdot}211$ ft, $A_1 = 0{\cdot}40$ (see figure 3*a*).

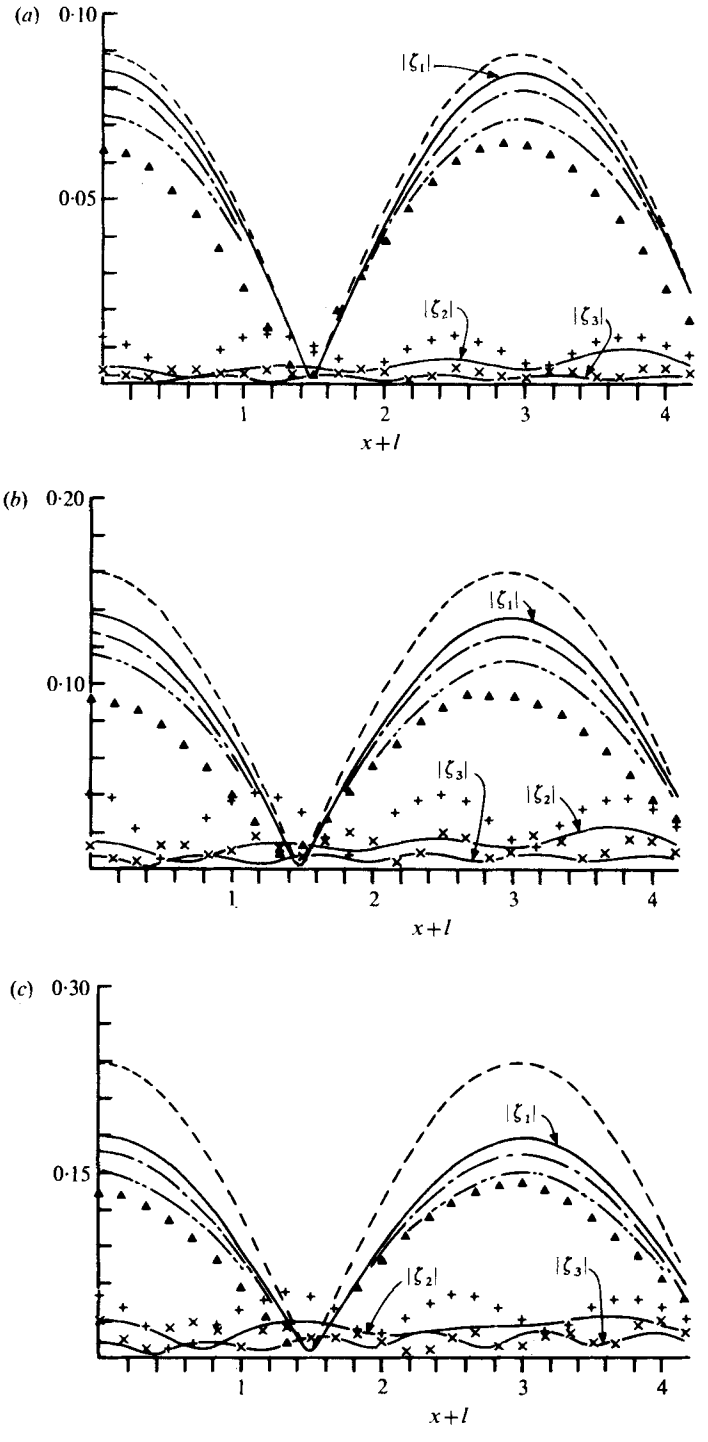

FIGURE 4. (a) $L = 4{\cdot}173$ ft, $A_1 = 0{\cdot}015$ (see figure 3a). (b) $L = 4{\cdot}173$ ft, $A_1 = 0{\cdot}027$ (see figure 3a). (c) $L = 4{\cdot}173$ ft, $A_1 = 0{\cdot}040$ (see figure 3a).

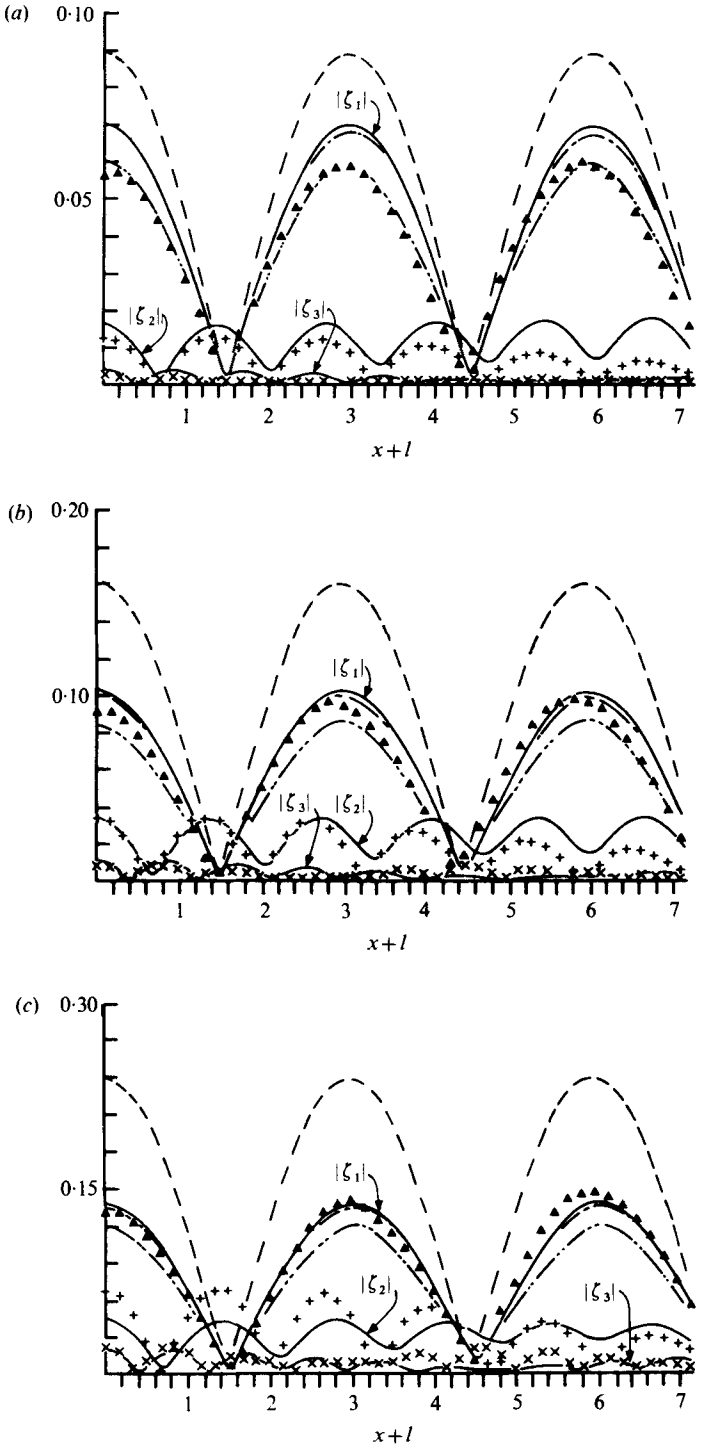

FIGURE 5. (*a*) $L = 7{\cdot}136$ ft, $A_1 = 0{\cdot}015$ (see figure 3*a*). (*b*) $L = 7{\cdot}136$ ft, $A_1 = 0{\cdot}027$ (see figure 3*a*). (*c*) $L = 7{\cdot}136$ ft, $A_1 = 0{\cdot}040$ (see figure 3*a*).

l \ $\lvert A_1\rvert/h$	0·015	0·027	0·040
1·227 $n = 0$	0·088 0·005, 0·013	0·139 0·005, 0·021	0·193 0·005, 0·029
4·230 $n = 1$	0·063 0·019, 0·009	0·092 0·019, 0·014	0·134 0·019, 0·020
7·233 $n = 2$	0·056 0·032, 0·008	0·091 0·032, 0·014	0·131 0·032, 0·020

TABLE 2. Values of $|T_1|/h$, c_v and c_e for nine resonant cases. In each box the numbers represent

$\lvert T_1\rvert/h$
c_v, c_e

.

of reducing the amplification of ζ_1/A_1 and increasing ζ_2 and ζ_3. The reduction of linear resonance by spreading energy to higher harmonics is greater for a longer bay; this is in accord with the fact that a longer bay allows more space for nonlinear interaction to manifest itself. Compared with experiments, the inviscid predictions are excellent for the longest bay, but less good for the shortest, again confirming that nonlinearity plays a more dominant role in longer bays. Note that the maximum values of $|\zeta_1|$ in these figures give the values of ϵ directly, the largest measured value being $\epsilon = 0{\cdot}19$ (figure 3*c*).

The calculated second and third harmonics deviate rather significantly in percentage from the measured values in figures 3 and 4 where the amplitudes of these harmonics are small, but the agreement is not bad in figure 5, where the second harmonic is appreciable. Aside from possible experimental inaccuracy, two shortcomings of the numerical theory may contribute to this deviation. One is the magnitude of μ^2, which may be large enough to call for a theory accurate up to $O(\mu^4)$. One is our averaging approximation of the impedance condition which ignores the details of the flow near the entrance. The latter simplification affects the accuracy of Z_n which in turn affects the frequency of the resonant peaks, especially for higher values of n.

To get a quantitative idea of the three kinds of losses involved in our experiments, we list in table 2 the estimated values of the boundary-layer damping rate c_v by equation (A 4) and the entrance separation damping rate c_e by (A 5*b*) in the appendix. Under the circumstances,

$$c_e = \frac{4}{3\pi} f \frac{gk^2}{\omega^2} |T_1| = 0{\cdot}15|T_1|/h,$$

where (T_1/h) is taken to be the measured values also shown in table 2. The radiative loss factor which is proportional to P_R in equation (A 1) is $c_Q = ka \cong 0{\cdot}17$ in all cases. It clearly shows that entrance loss overshadows the boundary-layer loss for shorter bays and large amplitudes, while the reverse is true for longer bays.

In figure 3 for the shortest bay ($n = 0$) nonlinearity and entrance loss are of comparable importance while boundary-layer loss is insignificant. For the medium-length

bay ($n = 1$) all three factors are comparable (figure 4). For the longest bay ($n = 2$, figure 5) nonlinearity is dominant and entrance loss is the least important, while boundary-layer loss appears to be correctly accounted for for the smallest amplitude (figure 5*a*), but is over-estimated for larger amplitudes (figures 5*b*, *c*). More accurate comparison would require a theory which accounts for nonlinearity, dispersion and viscosity more fully than is attempted here, and more extensive experiments. The present work has perhaps served the purpose of affirming the role of nonlinearity in shallow-harbour resonance.

6. Concluding remarks and possible improvements

We have used the Boussinesq equations to study resonant oscillations in a rectangular bay due to incident waves. Approximations suitable for small bay width lead to a nonlinear boundary-value problem for the bay. From calculated and experimental results we may conclude that for a short bay, entrance losses can be more important than nonlinearity, but for a long bay the reverse is true. This conclusion should hold in some prototype bays because the friction coefficient f used here to estimate entrance loss remains relevant in order of magnitude. We believe that for a narrow entrance, the argument for linearizing the ocean while keeping the bay nonlinear may be extended to more general harbours. Indeed, this simplification may be important for devising more ambitious numerical techniques for harbours of general shape and variable depth, since it permits one to limit the costly nonlinear computations to a finite region within the harbour.

Several improvements of the numerical theory of this paper may be considered for the future. First, when nonlinearity ϵ or the bay length is still greater than those studied herein, many more higher harmonics can be expected and the method in § 3 can then be costly. A more efficient approach is to use the fact that the harmonics vary nearly sinusoidally in space with slowly varying amplitude, see (3.4*b*). By essentially following a method of Bryant (1973) for progressive waves, we may assume the nth harmonic to be

$$\zeta_n(x) = c_n^+(x)\exp(inx) + c_n^-(x)\exp(-inx), \tag{6.1}$$

where c_n^+ and c_n^- are slowly varying in x (scale $\sim \epsilon^{-1}$). It can be shown that $c_n^\pm$ satisfies

$$\pm\frac{dc_n^\pm}{dx} - \frac{i\mu^2}{6\epsilon}n^3 c_n + \tfrac{1}{4}i\sum_s (n+s)\,c_s^\pm\, c_{n-s}^\pm = 0. \tag{6.2}$$

From (2.26) the boundary conditions on $c_n^\pm$ are

$$c_n^+(-l)\exp(-inl) - c_n^-(-l)\exp(inl) = 0, \tag{6.3a}$$

$$c_n^+(0) + c_n^-(0) = A_n + \frac{n^2}{k_n^2}Z_n(c_n^+(0) - c_n^-(0)). \tag{6.3b}$$

[See Rogers (1977) for derivation.] The method of complementary functions in § 3.3 can be adapted here with some modification. The advantage of solving (6.2) and (6.3) is that the discretizing interval can be much coarser than that of § 3.3 for the same accuracy.†

† Comments of a referee led to this statement.

The second improvement should be in the matching conditions at the bay entrance where the adopted impedance condition becomes progressively poor for higher harmonics. A simple and rigorous remedy is not apparent, however.

In tsunami studies if transients are put aside the dominant wavelengths are so long that μ^2 and δ are usually much smaller than in our experimental harbours. For example, take $2a = 100\,\mathrm{m}$, $h = 20\,\mathrm{m}$ and $L = 5000\,\mathrm{m}$; the first three linear resonant modes are near $\omega L/(gh)^{\frac{1}{2}} = 1{\cdot}52$, $4{\cdot}59$ and $7{\cdot}68$, corresponding to wave periods of 24·6, 8·14 and 4·87 min respectively. The corresponding μ^2 and δ are extremely small: $\mu^2 = 3{\cdot}7 \times 10^{-5}$, $3{\cdot}4 \times 10^{-4}$ and $9{\cdot}4 \times 10^{-4}$ and $\delta = 0{\cdot}015$, $0{\cdot}046$ and $0{\cdot}077$, respectively. In these cases, Airy's non-dispersive theory would be adequate in the harbour. It would also be of interest to study the more nonlinear equations of Su & Gardner (1969) which are valid for small μ^2 but arbitrary ϵ. For some small and shallow harbours, nonlinear effects enhanced by linear resonant excitation are conceivable even for the relatively short swells but a three-dimensional theory would be necessary and worthwhile.

Steven Rogers wishes to thank the Fannie and John Hertz Foundation for a fellowship during his graduate study at M.I.T. Both authors thank the Fluid Dynamics Program, Office of Naval Research, for supporting the research.

Appendix. Procedure for estimating real-fluid effect on the first harmonic

For the purpose of comparison let us first estimate the average power loss by radiation

$$P_R = 2ah\frac{\omega}{2\pi}\int_0^{2\pi} dt\rho g\zeta^R(0,t)\,u(0,t) = \rho gah\left(\frac{gk}{\omega}\right)(ka)|T_1|^2\sin 2kL, \tag{A 1}$$

where the linear theory has been used.

By using standard theory for the power loss inside the boundary layer (see e.g. Batchelor 1967, pp. 355 ff.), the total viscous power loss along the entire wall surface of the bay is easily found to be

$$P_v = 2(a+h)\int_{-L}^{0}\frac{dP_v}{dA}\,dx = \frac{1}{2\delta_v}\rho\nu\left|\frac{gkT_1}{\omega}\right|^2(a+h)L. \tag{A 2}$$

Thus the ratio of viscous damping to radiation damping, which must be equal to the ratio of the corresponding damping factors, c_v/c_R, is

$$c_v/c_R = P_v/P_R = \frac{(a+h)\,\delta_v L}{4ha^2}\operatorname{cosec}^2 kL. \tag{A 3}$$

At resonant peaks, $kL \cong (m=\frac{1}{2})\pi$. For our dimensions,

$$c_v/c_R = P_v/P_R \cong (m+\tfrac{1}{2})(7{\cdot}88\times 10^{-2}), \tag{A 4}$$

which can be nearly 20% for the highest mode ($m = 2$) tested. (See table 2.)

For damping effect due to flow separation at the harbour entrance, we follow Ingard (1970), Ito (1970), Miles (1974), Ünlüata & Mei (1975) and Miles & Lee (1975). We adopt the empirical formula that, across the entrance $x = 0$, the free surface suffers a jump which is quadratic in the local mean velocity. It is also known that the

primary consequence of this loss is on the fundamental harmonic which can be accounted for by an equivalent linear loss formula,

$$\zeta(0^-,t)-\zeta(0^+,t) = c_e u(0,t) \tag{A 5a}$$

with

$$c_e = (8/3\pi) f|U_1|/2g, \tag{A 5b}$$

where U_1 is the complex amplitude of the first harmonic. The friction factor f may be estimated by averaging the steady flow values of sudden expansion ($<1{\cdot}0$) and contraction ($<0{\cdot}4$). Combining (A 5) and (2.21) we get

$$\zeta_1(0^-) = A_1 + (Z_1 + c_e) U_1, \tag{A 6}$$

for the first harmonic.

The linearized approximation corrected for entrance loss is given by (2.8) with T_1 replaced by

$$T_{1f} = A \left\{ \left[\cos k_1 L + \frac{gk_1}{\omega} (\operatorname{Im} Z_1) \sin k_1 L \right] - \frac{igk_1}{\omega} \sin k_1 L \left[\operatorname{Re}(Z_1) + \frac{4}{3\pi} \frac{k_1}{\omega} f |T_{1f}| \right] \right\}^{-1}. \tag{A 7}$$

In particular, at resonance (2.10) still holds, and one gets

$$|T_{1f}/T_1| = [-1 + (1+4\alpha)^{\frac{1}{2}}]/2\alpha, \tag{A 8}$$

with

$$\alpha \equiv \frac{4}{3\pi} \frac{k_1}{\omega} f T_1 (\operatorname{Re} Z_1)^{-1}, \tag{A 9}$$

where T_1 is the inviscid resonant amplitude according to the linearized theory, i.e. (2.9).

In our experiments the corners of the model bay are slightly rounded with an approximate radius of curvature of $\frac{1}{2}$ in. Therefore, we have taken a friction coefficient $f = 0{\cdot}35$ which is half the maximum steady-state value.

Summarizing, for each resonant case we first incorporate entrance friction into the first harmonic by replacing $\operatorname{Re} Z_1$ with $c_R + c_e$ in the impedance condition (3.4) and then proceed with the numerical solution. The resulting solution, T_1', is then corrected for boundary-layer damping also by the following estimate:

$$T'' = T_1' \frac{c_R + c_e}{c_R + c_e + c_v} \quad \text{at resonance,} \tag{A 10}$$

with c_v/c_R given by (A 4).

REFERENCES

Batchelor, G. K. 1967 *An Introduction to Fluid Dynamics*, pp. 353–358. Cambridge University Press.

Berkhoff, J. C. W. 1972 Computation of combined refraction–diffraction. *Proc. 13th Coastal Engng Conf. A.S.C.E.*, pp. 471–490.

Bowers, E. C. 1977 Harbour resonance due to set-down beneath wave groups. *J. Fluid Mech.* **79**, 71–92.

Bryant, P. J. 1973 Periodic waves in shallow water. *J. Fluid Mech.* **59**, 625.

Chen, H. S. & Mei, C. C. 1974 Oscillation and wave forces in a man-made harbor in the open sea. *Proc. 11th Symp. Naval Hydrodyn.*, pp. 573–594.

Collins, J. I. 1963 Inception of turbulence at the bed under periodic gravity waves. *J. Geophys. Res.* **68**, 6007–6014.

Hwang, L. S. & Tuck, E. O. 1970 On the oscillation of harbours of arbitrary shape. *J. Fluid Mech.* **42**, 447–464.

INGARD, U. 1970 Nonlinear distortion of sound transmitted through an orifice. *J. Acoust. Soc. Am.* **48**, 32–33.

ITO, Y. 1970 On the effect of tsunami-breakwater. *Coastal Engng in Japan* **13**, 89–102.

JONSSON, I. G. & CARLSEN, N. A. 1976 Experimental and theoretical investigation in an oscillatory turbulent boundary layer. *J. Hydraul. Res.* **14**, 45–60.

KEULEGAN, G. H. 1959 Energy dissipation in standing waves in rectangular basins. *J. Fluid Mech.* **6**, 33.

LEE, J. J. 1971 Wave-induced oscillations in harbours of arbitrary geometry. *J. Fluid Mech.* **45**, 375–394.

LONGUET-HIGGINS, M. S. & STEWART, R. W. 1964 Radiation stresses in water waves; a physical discussion with applications. *Deep-Sea Res.* **11**, 539–562.

MILES, J. W. 1974 Harbor seiching. *Ann. Rev. Fluid Mech.* **6**, 17–35.

MILES, J. W. & LEE, Y. K. 1975 Helmholtz resonance of harbours. *J. Fluid Mech.* **67**, 445–464.

MILES, J. W. & MUNK, W. H. 1961 Harbor paradox. *J. Waterways Harbors Div. A.S.C.E.* **87**, 111–130.

MORSE, P. M. & FESHBACK, H. 1953 *Methods of Theoretical Physics*, vol. I, pp. 814–815. McGraw-Hill.

ROBERTS, S. M. & SHIPMAN, J. S. 1972 *Two-Point Boundary Value Problems: Shooting Methods.* Elsevier.

ROGERS, S. R. 1977 Finite amplitude harbor oscillations: theory and experiment. Sc.D. thesis, Department of Physics, Massachusetts Institute of Technology.

SU, C. H. & GARDNER, C. S. 1969 Korteweg–de Vries equations and generalizations. III. Derivation of Korteweg–de Vries equation and Burgers equation. *J. Math. Phys.* **10**, 536–539.

ÜNLÜATA, U. & MEI, C. C. 1973 Long wave excitation in harbors – an analytical study. *Parsons Lab. M.I.T. Tech. Rep.* no. 171.

ÜNLÜATA, U. & MEI, C. C. 1975 Effects of entrance loss on harbor oscillations. *J. Waterways, Harbors Coastal Engng Div. A.S.C.E.* **101**.

YOUNG, D. M. & GREGORY, R. T. 1973 *A Survey of Numerical Mathematics.* Addison–Wesley.